

Genetic Variations in SNCA Gene and Their Potential Therapeutic Implications for Parkinson's Disease

Yaghsha Javed¹, Muhammad Saleem^{1*}, Kainat Ramzan^{2*}, Hamna Tariq¹, Sadia Javeed³, Hafiz Abdul Moeed⁴

¹Department of Molecular Biology, Faculty of Life Sciences, University of Okara, Punjab, Pakistan

²Department of Biochemistry, University of Okara, Punjab, Pakistan

³Fatima Memorial College, Lahore, Punjab, Pakistan

⁴Faculty of Veterinary Science, University of Agriculture Faisalabad, Punjab, Pakistan

*Correspondence Author

DOI: <https://dx.doi.org/10.47772/IJRISS.2024.8110259>

Received: 16 November 2024; Accepted: 23 November 2024; Published: 23 December 2024

ABSTRACT

Genetic variations play a crucial role in disease pathogenesis and serve as key biomarkers in SNP analysis. Alpha-synuclein (SNCA), a presynaptic protein involved in neuronal plasticity, is implicated in Parkinson's disease through its abnormal accumulation in Lewy bodies and mutations in the α -synuclein gene. The nsSNPs are known to account for over 50% of genetic disorders, highlighting their importance in the molecular mechanisms underlying PD. In this study, sequence and structure-based web tools were employed to analyze SNCA mutations and their impact on the target protein. We identified disease-associated nsSNPs and predicted structural changes induced by these mutations. Molecular docking studies on both wild-type and mutant SNCA proteins were conducted using the PyRx algorithm. Our results revealed 20,268 SNPs in the SNCA gene regions, only 17 nsSNPs were found to be deleterious and disease-associated. The SNCA protein structure was modeled using the Swiss Model (2kkw.1.A), and model accuracy was evaluated using the SAVES server. Our analysis identified G36S and P138H missense mutations with significant deleterious effects, as indicated by their high RMSD values. Docking studies further highlighted Benazepril (-5.6), Rutin (-6.8), Hesperidin (-7.1), Cilazepil (-5.7), and Ketoconazole (-5.8) as promising candidates for binding with SNCA protein complexes. This study underscores potential therapeutic candidates and provides a foundation for exploring targeted treatments for PD through validation of the identified compounds and further nsSNP analysis. However, further experimental validation and clinical trials are needed to assess their efficacy and safety in PD treatment.

Key Words: DJ1, LRRK2, nsSNP, PD, PINK1, SIFT, SNCA, SNP

INTRODUCTION

Parkinson's disease (PD) is a progressive neurological disorder considered by motor symptoms (bradykinesia, rigidity, and tremors) and with non-motor symptoms (depression and cognitive decline). While 85-90% of PD cases are sporadic, with no clear genetic cause or family history and the remaining 10-15% are familial form (Dorsey & Bloem, 2024). These mutations are associated with an inherited form of PD, often presenting at an earlier age and exhibiting distinct symptom patterns and disease progression (Binotti, Jahn, & Pérez-Lara, 2021). Protein aggregation plays a critical role in PD, particularly in the SNCA gene, which encodes the alpha-synuclein protein. Mutations in PARK7 (DJ-1), PINK1, and PRKN (parkin) disrupt mitochondrial function and cellular stress responses, contributing to neurodegeneration. Additionally, mutations in LRRK2 are linked to disturbances in cellular processes, particularly within nerve cells, further exacerbating the PD progression (Bloem, Okun, & Klein, 2021). Studies have identified 25 variants of the PARK7 gene, including significant

mutations such as L166P and L172Q. These mutations lead to instability in the DJ-1 protein and increased oxidative stress, both of which contribute to PD development (Skou, Johansen, Okarmus, & Meyer, 2024).

Moreover, PINK1 gene mutation affects the ATP-binding pocket and catalytic motifs and disrupts its ability to phosphorylate ubiquitin and activate PARKIN. The G386A and H271Q were shown to abolish PINK1 activity, resulting in mitochondrial dysfunction and contributing to PD disorder (Kumar et al., 2017). Over 200 mutations in the PRKN gene have been identified, and PD individuals exhibit symptoms such as bradykinesia, rigidity, and postural instability. Patients with PRKN-related PD generally experience a slower disease progression and show a better response to dopaminergic therapy compared to those with idiopathic PD (Menon et al., 2024). At least 30 mutations in the SNCA gene, including A53T, A30P, E46K, H50Q, and G51D, have been linked to Parkinson's disease. These mutations result in the accumulation of alpha-synuclein, which forms Lewy bodies a key pathological feature of PD disrupting neuronal function and promoting cell death (Guan et al., 2020; Watt, Meade, Williams, & Mason, 2022). However, genetic studies provide valuable insights into the molecular pathways potentially involved in all cases of PD (Weisheit et al., 2020). While these variants are relatively rare, they offer valuable insights into the fundamental disease mechanisms and have deepened our understanding of both familial and sporadic forms of PD (Reddy et al., 2024).

The SNCA gene, which encodes α -synuclein (α S) plays a fundamental role in the pathophysiology of autosomal dominant PD variants (Lim & Klein, 2024), that are frequently associated with non-motor symptoms, including cognitive decline (Magistrelli, Contaldi, & Comi, 2021). In addition, immune responses associated with α -synuclein highlight an immunological component in PD conditions, involving both inherited and sporadic forms of PD (Brás, Gibbons, & Guerreiro, 2021). The α -synuclein is primarily localized in presynaptic terminals, where it regulates dopamine and is involved in synaptic vesicle trafficking and maintaining synaptic integrity. Although predominantly expressed in the brain, and peripheral tissues (heart, skeletal muscle, and pancreas), its presence in blood components has raised its potential as a biomarker for Parkinson's disease (Sharma et al., 2019; Wassouf et al., 2018).

The human SNCA gene spans 114,206 bp and is mapped on chromosome 4 (4q21) which consists of 6 coding exons and 2 non-coding exons. It has a total transcript length of approximately 3,041bp by encoding a protein of 140 amino acids, with a molecular weight of about 14.5 kDa (Fakhree et al., 2021). The structure of α -synuclein consists of three distinct regions, including the N-terminal lipid-binding α -helix (residues 1–60), which interacts with the non-amyloid beta component (NAC) domain of phospholipids (residues 61–95) and is responsible for amyloid aggregation, and the C-terminal acidic domain (residues 96–140), which adopts a random helical structure. Alterations in the N-terminal region are particularly significant, as they are involved in protein stability and contribute to the pathogenesis of neurodegenerative diseases and other synucleinopathies (Du et al., 2021).

Moreover, A53T, A30P, E46K, H50Q, G51D, and A53E variants lead to abnormal protein aggregation that impairs neuronal function and contributes to PD by disrupting cellular characteristics and promoting inflammatory responses (Morato Torres et al., 2020). Epigenetic factors, such as the methylation of the SNCA gene, can influence its expression. For example, increased binding of methyl-CpG binding protein 2 (MeCP2) to specific sites in the gene can downregulate alpha-synuclein (α S) production. Conversely, the absence of MeCP2 binding results in elevated levels of the protein (Marsal-García et al., 2021). The single nucleotide polymorphisms (SNPs) and repeat expansions were linked to altered SNCA protein expression levels and increased susceptibility to PD. This highlights the complex interplay between genetic factors and disease manifestation. Overall, mutations in SNCA and their impact on the native protein dynamics are crucial for understanding PD pathology and identifying potential therapeutic targets.

The present study aims to study the association between the SNCA gene and PD using computational methods. It will examine the functional analysis of non-synonymous SNPs linked to the SNCA gene, focusing on identifying disease-causing SNPs and assessing their impact on the target protein. Homology modeling, structural analysis, and molecular docking studies will be performed using various bioinformatics approaches. Integrating convolutional neural networks (CNNs) and deep learning techniques offers enhanced precision and efficiency, shaping the future of computational strategies for Parkinson's disease treatment.

MATERIALS AND METHODS

Retrieving SNCA data

The human SNCA gene, variation viewer, and protein sequence were attained from NCBI (<https://www.ncbi.nlm.nih.gov/search/all/?term=SNCA>), UniProt (<https://www.uniprot.org/uniprotkb/P37840/entry>), and Ensemble genome browser (http://asia.ensembl.org/Homo_sapiens/Gene/Summary) (Brás et al., 2021).

Deleterious Variants Prediction

Various bioinformatics tools have been developed to assess the potential functional impacts of polymorphisms. SNPnexus (<https://www.snp-nexus.org>) also incorporates additional tools, including Sorting Intolerant From Tolerant (SIFT) and PolyPhen, for more comprehensive predictions (J. Wang et al., 2022). SIFT classifies the variants into deleterious and tolerated, based on a tolerance score and those with a score ≤ 0.05 are considered to be deleterious (Shaik et al., 2023). PolyPhen labels the results as a benign, possibly damaging, or probably damaging score that ranges from 0 to 1, with 0 indicating benign and 1 indicating the probably damaging effect (Antonova et al., 2024). Additionally, PolyPhen-2 (<http://genetics.bwh.harvard.edu/pph2>) automatic tool to predict possible impact on human protein (Wright et al., 2023). PANTHER (<http://www.pantherdb.org/tools/csnpscoreform.jsp>) estimates the particular non-synonymous coding SNP to cause a functional impact on protein (Thomas et al., 2022). MutPred2 (<http://mutpred2.mutdb.org>) web server predicts the pathogenicity of coding sequence mutations, classifying them as neutral or disease-associated. It assigns a "pathogenic mutation" score between 0.5 and 1.0, with higher values indicating a greater likelihood of the mutation being pathogenic (Yazar & Özbek, 2021). VannoPortal (<http://www.mulinlab.org/vportal/index.html>) is a variant annotation database that integrates genome-wide variant annotations and prediction scores from various biological domains (J. Wang et al., 2022).

Disease associating Variants and Stability Analysis

SNPs & GO (<https://snps-and-go.biocomp.unibo.it/snps-and-go/>) (Bouqdayr et al., 2023), Meta-SNP (<https://snps.biofold.org/metasnps/pages/methods.html>) (Khalid & Naveed, 2022) and SUSPECT (www.sbg.bio.ic.ac.uk/suspect) a Disease-Susceptibility-based SAV Phenotype Prediction algorithms (Tanshee, Mahmud, Nabi, & Sayem, 2024), that are utilized to identify disease-associated nsSNPs by analyzing the impact of single-point protein variations. In these tools, an output value greater than 0.5 is considered indicative of a disease-associated mutation, suggesting a higher likelihood of causing disease. Conversely, a value less than 0.5 is classified as neutral, implying the mutation is unlikely to significantly impact protein function or be associated with disease [26].

Moreover, MU-Pro (<http://mupro.proteomics.ics.uci.edu>) (Keskin Karakoyun et al., 2023). i-Stable (<http://predictor.nchu.edu.tw/iStable/about.php>) (Beg, Hejazi, Thakur, & Athar, 2022) and DynaMut2 (<https://biosig.lab.uq.edu.au/dynamut2>) predicts changes in protein stability upon mutations in single amino acid residues using a support vector machine (Rodrigues, Pires, & Ascher, 2021). These assess the change in Gibbs free energy ($\Delta\Delta G$) to determine whether a mutation stabilizes or destabilizes a protein, with positive $\Delta\Delta G$ indicating stabilization and negative $\Delta\Delta G$ suggesting destabilization. They also analyze vibrational entropy changes ($\Delta\Delta S$) to evaluate how mutations affect protein flexibility.

Gene expression analysis

The Genotype-Tissue Expression (GTEx) portal (<https://www.gtexportal.org/home>) provides comprehensive information on gene expression across various human tissues. This analysis helps identify tissue-specific expression patterns and variations, offering insights into the gene's potential role in specific conditions or diseases (Costa, 2022).

SNCA model prediction

Using SWISS-MODEL (<http://swissmodel.expasy.org>), three-dimensional structures of both wild-type and mutant proteins were constructed to evaluate their structural stability (Banerjee, Santra, & Maiti, 2020). The

initial step in reconstructing the natural structure of the SNCA protein involved employing homology modeling method (Jumper et al., 2021). PyMOL (<https://pymol.org/2>) was utilized to modify specific amino acids and visualize the 3D structure of the SNCA protein (Wayment-Steele et al., 2024). The structural refinement was attained using the Galaxy Refine web-based algorithm (<https://galaxy.seoklab.org/cgi-bin/submit.cgi?type=REFINE>). Moreover, the QMEAN (<https://swissmodel.expasy.org/qmean>) tool evaluates protein model quality through geometrical analysis and comparative assessments.

Moreover, ProSA-web (<https://prosa.service.came.sbg.ac.at/prosa.php>) is widely employed for refining and validating experimental protein structures (Huang et al., 2023). The SAVES server (<https://saves.mbi.ucla.edu>) is a comprehensive platform for assessing and validating the accuracy of protein 3D structures. It integrates tools like PROCHECK, which evaluates stereochemical quality, 3D Verify, which compares the structure against known templates to check compatibility, and ERRAT, which analyzes non-bonded atomic interactions to identify errors. Together, these tools ensure the reliability of modeled protein structures for further analysis (Richard et al., 2022).

Comparison of model protein with mutant

TM-align (<https://zhanggroup.org/TM-align>) was employed to determine structural relationships among native proteins by calculating the TM-score and root mean square deviation (RMSD) (Sykes, Holland, & Charleston, 2022). The TM-score, which ranges from 0 to 1, quantifies the similarity between two protein structures, with a score closer to 1 indicating a high structural similarity and a score closer to 0 suggesting minimal resemblance. RMSD measures the average distance between corresponding atoms after structural alignment, providing an additional assessment of the structural differences (Sultana, Mou, Chatterjee, Faruk, & Hosen, 2024).

Mutant effect on protein structure

The variant effects were utilized to predict mutation clusters using the Mutation3D (<https://mutation3d.org/about.shtml>) server. Mutation3D helps in understanding the spatial distribution of mutations by analyzing the changes that impact protein conformation. By identifying regions where multiple mutations occur nearby, the server facilitates the identification of mutation hotspots that may play a crucial role in cancer progression (Ghasemi, Mahdavi, Maleki, Salahshourifar, & Kalayinia, 2022).

Blind Protein-Ligand Docking Approach

Compounds Optimization

To identify potential FDA-approved compounds, databases such as PubChem (<https://pubchem.ncbi.nlm.nih.gov>), and LOTUS (<https://lotus.naturalproducts.net>) can be used. These databases provide extensive information on available compounds, including their biological activity. The FDA-approved PD disorders include Levodopa, Carbidopa, Pramipexole, Entacapone, Tolcapone, Selegiline, Bzotropine, and Trihexyphenidyl. Other compounds, primarily used for anti-inflammatory or immunosuppressant effects, are currently being explored for their potential in PD therapy.

PyRx Program and Visualization

PyRx (Python Prescription) program (<https://pyrx.sourceforge.io>) is an open-source virtual screening software that integrates several tools for molecular docking, drug design, and virtual screening. It allows users to perform docking simulations to predict how small molecules interact with protein targets, aiding in drug discovery. The software can use the AutoDock Vina engine for docking simulations and also supports the management and visualization of ligand-protein interactions (Singh, Kumar, Lee, & Hong, 2024). Moreover, the Protein-Ligand Interaction Profiler (PLIP; <https://plip-tool.biotech.tu-dresden.de/>) was used to visualize 2D and 3D interactions, displaying the size and location of binding sites, hydrogen bonds, hydrophobic interactions, and bonding distances of the docked ligands (Kondratyev et al., 2022).

RESULTS

Retrieval of SNP IDs

Our study focused on the human SNCA gene, analyzing a total of 20,268 SNPs sourced from the NCBI, Ensembl, and Genome dbSNP databases. These SNPs were classified into various regions, as shown in **Figure 1a**. Specifically, there were 2,852 SNPs in the UTR region, 2,794 SNPs in the 3' UTR, 102,956 SNPs in the intronic region, 96,853 SNPs in the coding region, 243 SNPs in the exonic region, 7,903 SNPs in the non-coding region, 7,831 SNPs in the 3' downstream region, 1,841 SNPs in the 5' upstream region, 417 SNPs in the synonymous region, and 802 SNPs in the non-synonymous region. In this study, we worked on missense (nsSNPs) mutations present in the SNCA gene that alter protein function by causing single-point mutation.

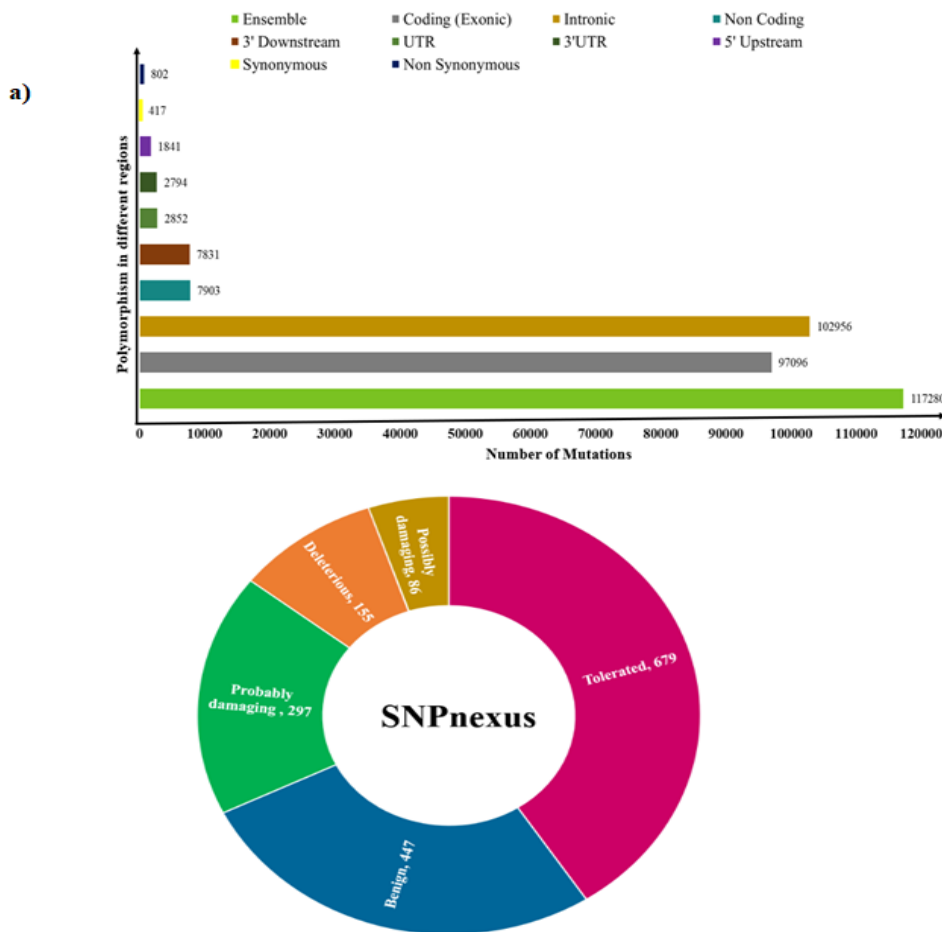


Figure 1. **a)** Bar plot evaluation of SNCA mutations found in different genomic regions **b)** Donut representation of nsSNPs by SIFT and PolyPhen.

Annotation of deleterious missense variants

Furthermore, SIFT predicted 679 missense mutations as deleterious and 155 as tolerated. PolyPhen analysis classified 297 nsSNPs as probably damaging, 86 as possibly damaging, and 447 as benign (**Figure 1b**). A comparison of the results from SIFT and PolyPhen revealed that all 17 common nsSNPs were identified as deleterious and probably damaging, as shown in **Table 1**. These K97N, P138S, G67R, L38P, A11S, V71A, V82A, E123K, P138H, T22I, V52A, V37F, K6N, P120L, T72M, G36S, and G73V were further analyzed using 12 different prediction servers to assess their impact and stability. The PANTHER predictions found that K97N, A11S, V71A, V82A, T22I, V37F, V52A, K6N, and G36S were classified as probably damaging, while 8 were predicted as probably benign. VannoPortal identified all 17 as missense variants. MutPred2 classified 13 of the nsSNPs as probably damaging, while 4 nsSNPs (P138S, P138H, E123K, and P120L) were considered possibly benign. PolyPhen2 predicted 15 nsSNPs as probably damaging, with A11S and V37F marked as possibly damaging, as shown in **Table 1**.

Table 1. Functional consequences of nsSNPs by various computational tools

rsID	AA	PolyPhen		SIFT		PANTHER		PolyPhen 2		VannoPortal	Mutpred 2	
		Score	Effect	Score	Effect	Effect	Pdel	Score	Effect	Effect	Effect	Score
rs1289807114	K97N	0.921	PD	0	D	PD	0.57	0.997	PD	Missense	PD	0.551
rs375682339	P138S	0.925	PD	0.01	D	PD	0.19	0.993	PD	Missense	PD	0.301
rs1418203843	G67R	0.932	PD	0	D	PD	0.19	0.992	PD	Missense	PD	0.879
rs1165791954	L38P	0.963	PD	0	D	PD	0.19	1	PD	Missense	PD	0.918
rs1219278381	A11S	0.965	PD	0.01	D	PD	0.57	0.887	PD	Missense	PD	0.589
rs777070190	V71A	0.971	PD	0.03	D	PD	0.57	1	PD	Missense	PD	0.756
rs1319839593	V82A	0.971	PD	0	D	PD	0.57	0.999	PD	Missense	PD	0.637
rs200056149	E123K	0.982	PD	0.02	D	PD	0.19	0.997	PD	Missense	Possibly benign	0.397
rs746232417	P138H	0.985	PD	0	D	PD	0.19	0.999	PD	Missense	Possibly benign	0.377
rs1273319141	T22I	0.986	PD	0	D	PD	0.57	0.999	PD	Missense	PD	0.757
rs1239518140	V52A	0.987	PD	0	D	PD	0.57	1	PD	Missense	PD	0.624
rs750745088	V37F	0.994	PD	0	D	PD	0.57	0.949	PD	Missense	PD	0.86
rs1188720061	K6N	0.994	PD	0	D	PD	0.57	1	PD	Missense	PD	0.586
rs1024288001	P120L	0.995	PD	0.02	D	PD	0.19	0.999	PD	Missense	Possibly benign	0.208
rs767026129	T72M	0.996	PD	0.01	D	PD	0.19	1	PD	Missense	PD	0.694
rs1342686707	G36S	0.998	PD	0	D	PD	0.57	0.999	PD	Missense	PD	0.821

*AA: Amino acid; D: Deleterious; PD: Probably Damaging

Association of nsSNPs with Disease and Stability

SNP & Go predictions, all nsSNPs were classified as disease-related, SuSpect identified 16 substitutions as disease-causing, with P120L being classified as neutral. Meta SNP predicted that G67R, L38P, V71A, T22I and G73V might be associated with diseases or disease conditions, while 12 nsSNPs were considered neutral, as detailed in **Table 3**. MuPro, i-Stable, and Dynamut 2 tools predominantly predicted a decrease in protein stability for most of the 17 nsSNPs, with the exceptions of rs767026129 and rs1261963254, which were generally associated with increased stability. MuPro indicated stability for T72M, while i-Stable predicted stability increases for T72V and G73V. Additionally, Dynamut 2 identified 5 SNPs as stabilizing, as detailed in **Table 3**.

Table 3. Identification of disease-associated nsSNPs and their effect on protein stability

rsID	AA	SNP & GO		Meta-SNP		Suspect		Mu- pro		i-stable		Dynamut 2	
		Effect	RI	Effect	RI	Effect	Score	Stability	Score	Effect	Score	Effect	Score
rs1289807114	K97N	D	8	N	2	D	60	↓	-0.59867	↓	0.582764	↑	0.62
rs375682339	P138S	D	7	N	6	D	39	↓	-0.82618	↓	0.633042	↓	-0.44
rs1418203843	G67R	D	9	D	3	D	82	↓	-0.43513	↓	0.698689	↓	-0.36
rs1165791954	L38P	D	10	D	3	D	71	↓	-2.07982	↓	0.809652	↓	-0.39

rs1219278381	A11S	D	9 N	1 D	79 ↓	-1.40066 ↓	0.71416 ↑	0.16
rs777070190	V71A	D	7 D	1 D	54 ↓	-1.32942 ↓	0.782387 ↓	-0.69
rs1319839593	V82A	D	5 N	3 D	44 ↓	-1.06964 ↓	0.6857 ↓	-0.61
rs200056149	E123K	D	5 N	7 D	26 ↓	-0.85637 ↓	0.718322 ↓	-0.07
rs746232417	P138H	D	7 N	5 D	42 ↓	-0.98165 ↓	0.631912 ↑	0.09
rs1273319141	T22I	D	9 D	2 D	80 ↓	-0.46921 ↓	0.647034 ↓	-0.09
rs1239518140	V52A	D	6 N	1 D	60 ↓	-1.80968 ↓	0.689347 ↓	-0.41
rs750745088	V37F	D	9 N	0 D	82 ↓	-1.00892 ↓	0.660921 ↓	-0.14
rs1188720061	K6N	D	8 N	0 D	45 ↓	-0.90636 ↓	0.703522 ↑	0.89
rs1024288001	P120L	D	8 N	6 N	16 ↓	-0.67645 ↓	0.671043 ↓	-0.14
rs767026129	T72M	D	8 N	2 D	37 ↑	0.129624 ↑	0.748936 ↑	0.31
rs1342686707	G36S	D	9 N	0 D	86 ↓	-0.66713 ↓	0.786414 ↓	-0.14
rs1261963254	G73V	D	9 D	3 D	73 ↓	-0.02374 ↓	0.610853 ↓	-0.79

*D:Disease; N: Neutral; ↓: Decrease; ↑: Increase

Tissue gene expression analysis

The violin plot illustrates the tissue-specific gene expression of SNCA (ENSG00000145335.15) across various human tissues, measured in TPM (Transcripts per Million). High expression of SNCA is observed in several brain regions, notably in the amygdala, caudate, and hippocampus, with median values exceeding 100 TPM and some samples reaching up to 300 TPM. This elevated expression in neural tissues reflects SNCA's critical role in the central nervous system, particularly in synaptic function, and highlights its association with PD. In addition to the brain, SNCA expression is also notably high in the uterus and vagina, with the uterus exhibiting the highest non-brain expression, surpassing 300 TPM. This suggests a potential role for SNCA in reproductive tissues, possibly related to cellular signaling or hormonal functions. Conversely, SNCA expression is minimal in tissues such as the thyroid, kidney, and gastrointestinal tract, indicating a limited role in these areas. Overall, the expression profile underscores SNCA's significant involvement in brain and reproductive tissues, supporting its known functions in neural processes and suggesting potential relevance in reproductive health. These findings warrant further investigation, particularly regarding tissue-specific diseases and cellular regulatory mechanisms linked to SNCA, as depicted in **Figure 2**.

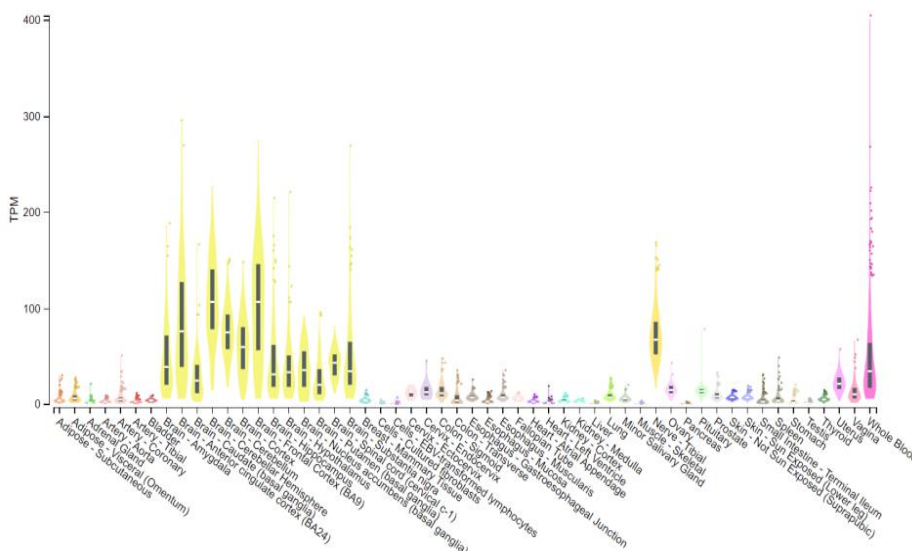


Figure 2. Tissue gene expression of SNCA interpreted by GTEX database

Homology modeling and structure conformation

The 3D structure of the target protein was not fully available, so we used homology modeling via the Swiss Model program. We identified 10 templates that exhibited 100% sequence identity with the query sequence. To assess the impact of mutations on protein stability, we selected the template 2kkw.1.A, which covers amino acids 1 to 140. This template is closely related to the micelle-bound alpha-synuclein structure and has a Global Model Quality Estimation (GMQE) score of 0.59. The native structure of the SNCA protein was generated using the 2kkw.1.A template and Chimera, as shown in **Figure 3a**. The model templates were verified using QMEAN and ProSA web. The model 2kkw.1.A, represented as a red star in **Figure 3b**, was assessed using these tools. QMEAN yielded a Z-score of -1.94, while ProSA web provided a score of -1.05 (**Figure 3c**), both indicating potential instability in the protein structure. A negative QMEAN and PROSAWEB Z-score suggests that the modeled protein structure may have a lower stability, demanding further evaluation and refinement.

To validate the model, a Procheck Ramachandran plot was generated by SAVESv6.1 to examine the Phi and Psi angle distribution of non-glycine and non-proline residues (**Figure 3d**). The plot categorizes residues based on their placement in quadrangles including red regions represent the most favored regions, while yellow regions denote allowed regions. Glycine residues are represented by triangles and all other residues by squares. For the 2kkw.1.A model, 97.40% of the residues were located within the core favored regions, 2.60% in allowed regions, and none in generously allowed or disallowed regions. This high proportion of residues in favorable regions indicates the model's high quality and structural reliability. The proteins associated with this model were downloaded along with their corresponding PDB files, and mutations were introduced using PyMOL. The G36S and P138H with high RMSD values (0.47 and 1.46) were particularly noted, indicating significant structural deviations that could impact the protein's function or stability as summarized in **Table 4**.

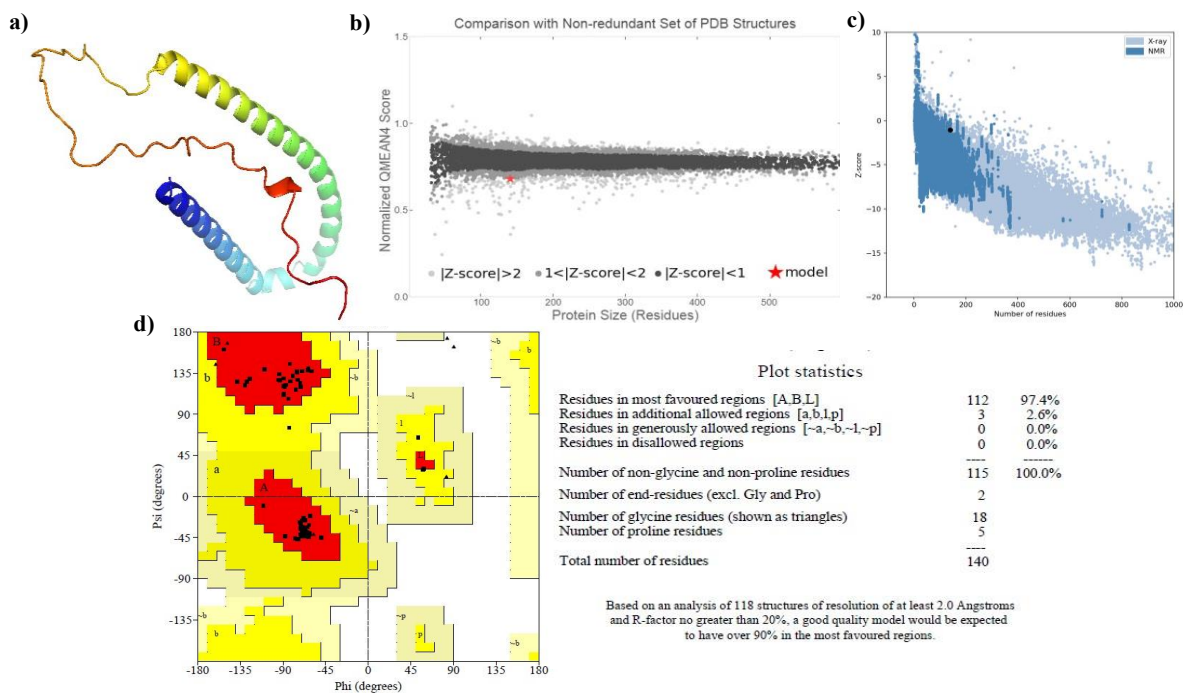


Figure 3. Structural modeling analysis a) Tertiary structure of SNCA protein, b) QMEAN analysis c) ProSA web of the native SNCA predicted model d) Statistics of model Ramachandran Plot by PROCHECK.

Structural Effect of Protein

Using the Mutation3D server, the 17 missense variants were observed to cluster within the SNCA protein structure as given in **Table 4**. Four nsSNPs (G67R, V71A, G73V, and T72M) formed a distinct cluster (marked in red), indicating a potential hotspot for structural or functional perturbations. The remaining 13 variants were linked to human genes and implicated as potential cancer-driving mutations. These findings highlight significant regions within the SNCA protein that could contribute to pathological mechanisms, as depicted in **Figure 4**.

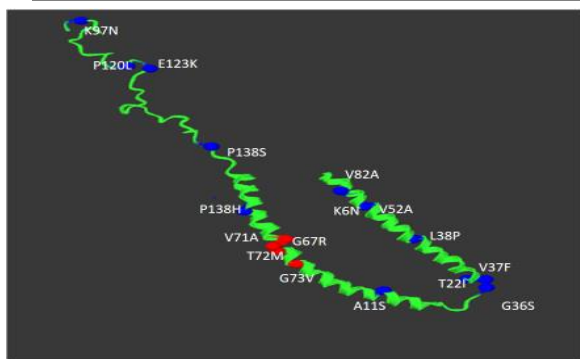


Figure 4. Structure predicted by mutation 3D by highlighting the changes in the SNCA gene.

Table 4. SAVESv6.1, TM align and mutation 3D analysis of native and mutant SNCA protein

Mutation 3D		ERRAT	Procheck				Verify 3D	TM ALIGN	
			Core	Allowed	Generously	Disallowed		TM Score	RMSD
Model		87.8788	97.40%	2.60%	0.00%	0.00%	27.14%		
K97N	Covered	92.1569	96.50%	1.70%	0.90%	0.90%	27.86%	0.9218	0.46
P138S	Covered	92.5532	98.30%	1.70%	0.00%	0.00%	19.29%	0.9915	0.41
G67R	Clustered	91.2621	95.70%	4.30%	0.00%	0.00%	18.57%	0.9905	0.43
L38P	Covered	89.3204	97.40%	2.60%	0.00%	0.00%	27.14%	0.9898	0.45
A11S	Covered	91.9192	97.40%	2.60%	0.00%	0.00%	15.00%	0.991	0.42
V71A	Clustered	95.9596	97.40%	2.60%	0.00%	0.00%	20.00%	0.9905	0.43
V82A	Covered	94.0594	98.30%	1.70%	0.00%	0.00%	15.71%	0.9912	0.42
E123K	Covered	94.1748	97.40%	2.60%	0.00%	0.00%	16.43%	0.9901	0.45
P138H	Covered	94.1324	97.40%	2.60%	0.00%	0.00%	15.71%	0.9899	1.45
T22I	Covered	93.0213	96.50%	3.50%	0.00%	0.00%	12.14%	0.9915	0.41
V52A	Covered	93.1373	96.50%	3.50%	0.00%	0.00%	22.86%	0.9914	0.41
V37F	Covered	91.3043	98.30%	1.70%	0.00%	0.00%	12.86%	0.9923	0.39
K6N	Covered	96.0396	98.30%	1.70%	0.00%	0.00%	22.86%	0.9903	0.44
P120L	Covered	91.8367	98.30%	1.70%	0.00%	0.00%	16.43%	0.9913	0.41
T72M	Clustered	89.7959	97.40%	2.60%	0.00%	0.00%	13.57%	0.991	0.42
G36S	Covered	96.7033	97.40%	2.60%	0.00%	0.00%	13.57%	0.9889	0.47
G73V	Clustered	93.1012	98.30%	1.70%	0.00%	0.00%	12.86%	0.9912	0.42

Ligand preparation and virtual docking studies

This study employed blind protein-ligand docking using the PyRx tool to investigate interactions between 35 selected ligands and the SNCA protein. These ligands were sourced from the PubChem and LOTUS databases, which provide comprehensive information, including ligand structures, biological properties, and docking data. The PyRx docking approach allowed for the unbiased identification of binding sites across the SNCA protein,

facilitating the analysis of potential interactions that could influence the protein's structure and function. This methodology supports the screening of promising candidates for further experimental validation in targeting SNCA-related PD mechanisms. Ligands targeting SNCA aim to modulate expression, prevent aggregation, or enhance toxic aggregate clearance. Curcumin, quercetin, myricetin, and fisetin show promise for directly targeting SNCA aggregation. Drugs like levodopa & carbidopa alleviate PD symptoms by replenishing dopamine, addressing neuron loss caused by SNCA aggregation. Pramipexole mitigates aggregation effects by reducing oxidative stress and providing neuroprotection. Entacapone and Tolcapone support dopaminergic systems, while selegiline protects neurons via MAO-B inhibition. Benztropine & trihexyphenidyl manage motor symptoms without directly affecting SNCA.

Moreover, bioactive ligands with potential SNCA modulation include curcumin (aggregation inhibition and fibril disaggregation), quercetin (fibrillation inhibition and antioxidant support), and genistein (expression and aggregation modulation). Polyphenols like myricetin, catechin, and fisetin protect neurons, while flavonoids such as rutin, naringenin, and morin inhibit fibrillation and oxidative damage. Compounds silymarin and thymoquinone reduce oxidative stress and aggregation, and safranal and paeoniflorin offer neuroprotective and anti-inflammatory effects. Other ligands, such as ketoconazole and gentian violet, may modulate aggregation and clearance pathways, while dequalinium could address mitochondrial dysfunction. ACE inhibitors (cilazepiril, benazepril) may reduce neuroinflammation and vascular dysfunction, indirectly benefiting PD by mitigating SNCA-related neurodegeneration.

The results highlight compounds Ketoconazole, Rutin, Cilazepiril, Benazepril, Hesperidin, and Paeoniflorin as significant candidates based on their docking scores with both native and mutant (P138H and G36S) protein. Protein-ligand interaction profiling (PLIP) revealed unique interactions for each compound. Notably, Hesperidin demonstrated strong positioning within the SNCA binding pocket, driven primarily by van der Waals forces, indicating a stable interaction. Comparative analysis of native and mutant states, as summarized in **Table 5**, revealed significant differences in ligand binding, emphasizing the role of mutations in altering protein-ligand interactions.

Table 5. Top-ranked docking score of 35 compounds with native and mutant proteins

Ligands	Protein (Receptor)			Ligands	Protein (Receptor)		
	Model	K97N	G36S		Model	K97N	G36S
Levodopa	-4	-4	-3.9	Rutin	-6.8	-6.1	-6.8
Carbidopa	-4	-3.9	-4.1	Cilazepiril	-5.7	-5.2	-5.7
Pramipexole	-3.9	-3.7	-3.8	Morin	-5.6	-5.7	-5.6
Entacapone	-4.4	-4.1	-4.1	Fisetin	-6	-5.8	-6
Tolcapone	-4.9	-4.9	-4.9	Safranal	-4.4	-4.5	-4.5
Selegiline	-3.8	-3.5	-3.8	Sesamol	-3.7	-3.6	-3.7
Benztropine	-5	-4.9	-5	Silymarin	-7	-6	-5.8
Trihexyphenidyl	-4.9	-4.9	-5	Myricetin	-4.7	-5.6	-4.7
Dequalinium	-4.4	-3.7	-3.7	Catechin	-5.6	-5.6	-5.8
Ketoconazole	-5.8	-5.4	-5.8	Benzepril	-5.6	-5.4	-5.7
Gentian violet cation	-5.4	-5.1	-5.5	Naringenin	-5.7	-5.7	-5.7
Mycophenolic acid	-4.2	-4.3	-4.5	Thymoquinone	-4.3	-4.3	-4.4

Genistein	-4.8	-5.1	-4.8	Hesperidin	-7.1	-6.4	-7
Curcumin	-5.1	-4.9	-5.1	Quercetin	-4.9	-5.5	-4.9
Chrysin	-5.8	-5.7	-5.8	Paeoniflorin	-5.5	-5.6	-5.1

The docking contacts between the drug Ketoconazole and the wild-type (SNCA) protein are shown in **Figure 5** and two key interactions involving hydrophobic groups were identified (**Table 6**). These hydrophobic interactions could contribute to the stabilization of the binding between Ketoconazole and the SNCA protein, that may influence α -synuclein aggregation or neurodegeneration in PD (Palani, Deivasigamani, Piramanayagam, & Murthy, 2023).

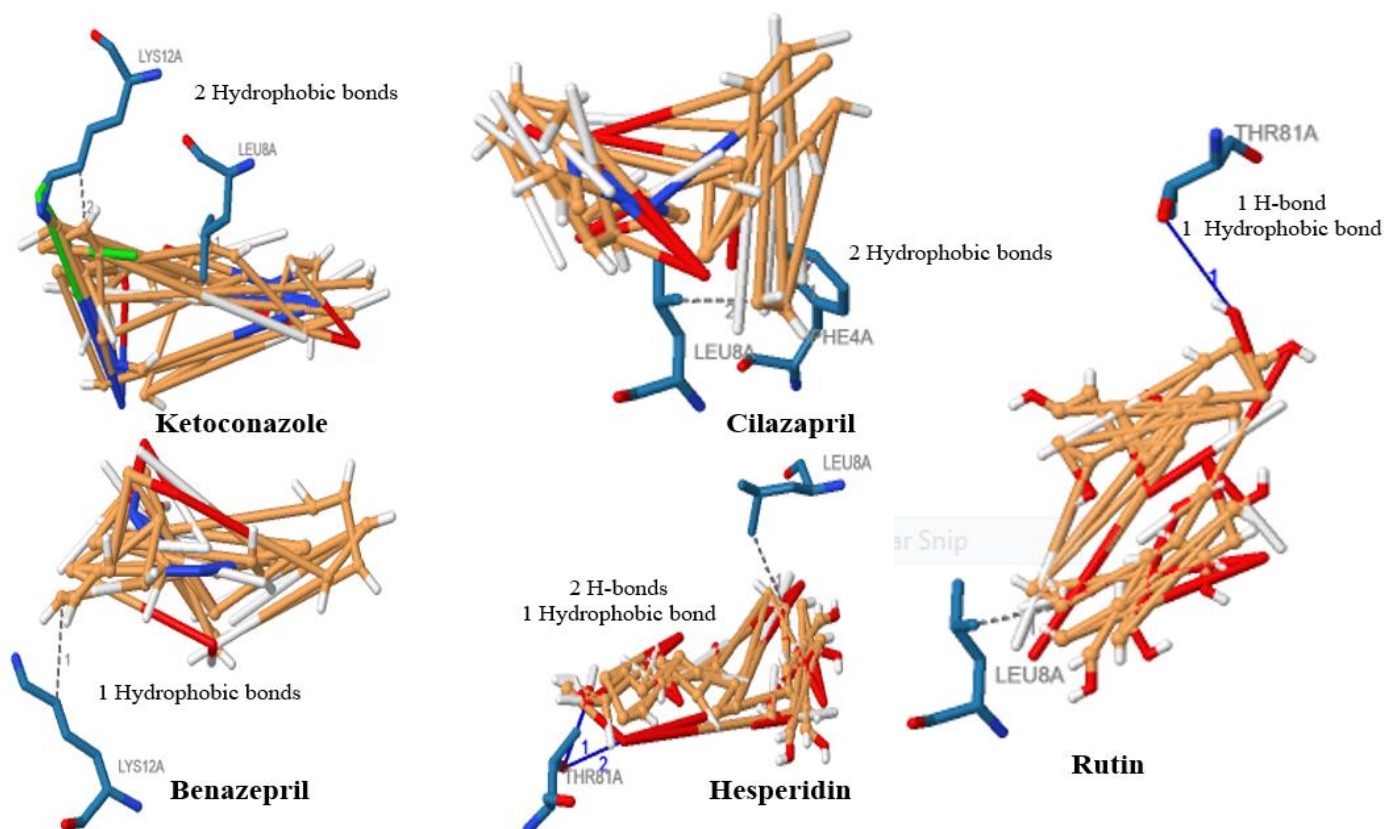


Figure 5. PLIP visualization of native SNCA with the highest docking score compounds

Our findings revealed that the wild-type SNCA protein interacts with Rutin, forming one hydrogen bond and one hydrophobic interaction, as detailed in **Table 6**. Rutin, a quercetin glycoside with known neuroprotective properties, shows potential in Parkinson's disease (PD) by modulating SNCA gene activity (Grewal et al., 2021). The docking interactions between Cilazapril and the SNCA protein are outlined in **Table 6** from two hydrophobic contacts with the protein, highlighting its potential role in modulating alpha-synuclein function, and offering a promising avenue for PD-related therapeutic research (Paulékas et al., 2024). Moreover, Benazepril is predicted to form one hydrophobic interaction. Benazepril, commonly known as an angiotensin-converting enzyme (ACE) inhibitor, has been studied for its potential influence on the SNCA gene (Caramiello & Pirota, 2024).

Moreover, **Table 6** predicts the formation of two hydrogen bonds and one hydrophobic interaction of Hesperidin, a naturally occurring flavonoid found in citrus fruits, which has demonstrated neuroprotective properties in PD models (Wolff, 2023). The visual representation and detailed bond interactions between the selected compounds and the mutant SNCA protein were examined using the PLIP algorithm, providing insights into the specific binding modes. These interactions highlight the key residues involved and the nature of the interactions (hydrogen bonds, hydrophobic contacts, etc.), as summarized in **Table 7**. The mutation-induced alterations in interacting residues and binding patterns underscore the dynamic nature of the SNCA protein's binding pocket. These differences may impact the compounds' therapeutic efficacy and specificity,

suggesting that further studies, including molecular dynamics simulations, are crucial to refine these interactions for potential drug development.

Table 6. PLIP interacting residues of the target protein with highlighted compounds

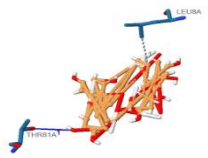
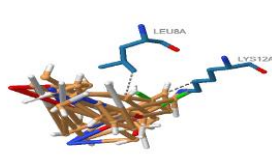

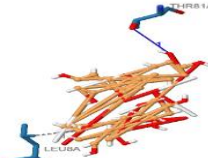
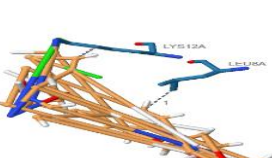
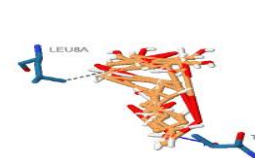
Ketoconazole	Hydrophobic	Residue	AA	Distance	Ligand Atom	Protein Atom
	1	8A	LEU	3.08	1044	62
	2	12A	LYS	2.29	1046	90
Rutin	Hydrophobic	Residue	AA	Distance	Ligand Atom	Protein Atom
	1	8A	LEU	3.24	1041	62
	H-Bond	Residue	AA	Distance H-A	Distance D-A	Donor Angle
	1	81A	THR	3.24	3.77	145.93
Cilazapril	Hydrophobic	Residue	AA	Distance	Ligand Atom	Protein Atom
	1	4A	PHE	3.16	1043	34
	2	8A	LEU	2.73	1040	62
Benazepril	Hydrophobic	Residue	AA	Distance	Ligand Atom	Protein Atom
	1	12A	LYS	3.58	1036	90
Hesperidin	Hydrophobic	Residue	AA	Distance	Ligand Atom	Protein Atom
	1	8A	LEU	3.27	1040	62
	H-Bond	Residue	AA	Distance H-A	Distance D-A	Donor Angle
	1	81A	THR	1.49	2.31	139.11
	2	81A	THR	2.18	2.72	113.42

DISCUSSION

Parkinson's disease (PD) is a complex neurodegenerative disorder primarily marked by motor symptoms such as bradykinesia, rigidity, and tremors, which arise from the degeneration of dopaminergic neurons in the substantia nigra (Legito & Andriani, 2023). It becomes more prevalent with age and is also influenced by environmental factors. Genetic research has identified over 200 genes associated with PD, leveraging large population studies and the investigation of rare Mendelian forms of the disease to uncover potential risk factors and causal genes. These studies have provided valuable insights into the genetic underpinnings of PD, helping to identify both common and rare genetic variations that may contribute to its development, and paving the way for more targeted diagnostic and therapeutic strategies (Kalia, 2024). Furthermore, SNP analyses in case-control studies have identified several variants in the SNCA gene (A53T and A30P) (Blauwendraat et al., 2021), including the dinucleotide repeats REP1 in the promoter region and the 3' UTR. These variants may enhance susceptibility by altering transcription factor binding sites, potentially impacting SNCA gene expression and contributing to the pathological aggregation of alpha-synuclein, a hallmark of PD (Matthews et

al., 2023).

Table 7. Visual Representation and bond interaction was examined by PLIP Algorithm

Ligands	Rutin	Ketoconazole	Hesperidin
G36S	1 H- Bond, 1 Hydrophobic	2 Hydrophobic	1 H- Bond, 1 Hydrophobic
Representations			
P138H	1 H- Bond, 1 Hydrophobic	2 Hydrophobic	2 H- Bond, 1 Hydrophobic
Representation			

The SNPs linked to the risk of PD are found across various populations and may impact microRNA binding sites, leading to changes in gene expression (Guo, Wang, Sun, & Liu, 2022). The SNCA polymorphisms in genes LRRK2, DJ1, PINK1, and Parkin are significant risk factors for PD (Liu, Singleton, Arribas-Bel, & Chen, 2021), and are commonly associated with early-onset PD and are often accompanied by severe non-motor symptoms, including cognitive decline (D’Addio et al., 2024). This study focuses on retrieving the FASTA sequence of the SNCA gene and utilizing computational tools to predict deleterious coding variants. The functional analysis aims to identify disease-causing SNPs and evaluate their impact on protein stability. Additionally, the 3D structure of the SNCA protein is predicted to analyze its structural integrity. To further explore the functional implications, protein-ligand blind docking is performed to investigate potential protein-ligand interactions.

By integrating these approaches, the study assesses the effects of mutations on the SNCA protein and their broader functional consequences. The present findings identified 17 nsSNPs as common according to SIFT and PolyPhen, all classified as deleterious and potentially damaging. Integrating tools such as PANTHER, Vannoportal, MutPred 2, and PolyPhen2, the analysis revealed that K97N, A11S, V71A, V82A, T22I, V37F, V52A, K6N, and G36S were probably damaging, while E123K, K6N, P138S, P138H, P120L, T72M, G73V, and G67R were predicted to be probably benign by PANTHER. Vannoportal annotated all 17 as missense variants. MutPred2 and PolyPhen2 indicated P138S, E123K, and P138H as possibly benign, with A11S and V37F classified as potentially damaging. SNP & Go classified P120L as neutral, while Meta SNP highlighted five mutations (G67R, L38P, V71A, T22I, and G73V) as potentially disease-associated. Protein stability analysis using i-Stable, Dynamut 2, and MuPro predicted that T72M was associated with higher stability according to MuPro, while i-Stable indicated increased stability for both T72M and G73V. In contrast, Dynamut 2 identified a decrease in stability for all 17 SNPs. These findings provide valuable insights into the structural and functional implications of these mutations.

Moreover, the Swiss Model generated 10 templates with 100% sequence identity, selecting template ID 2kkw.1.A for its similarity to the micelle-bound SNCA structure, covering amino acids 1-140 and a GMQE score of 0.59. Structural refinement and quality assessment of the model were performed, followed by the use of the PyRx tool to investigate ligand-protein interactions. Docking studies with both the wild-type and mutant SNCA yielded five unique conformations for each selected ligand, with a binding affinity (-kcal/mol) serving as a critical metric. Molecular docking, a structure-based drug design, predicts the binding conformations of small molecules to target sites, providing insights into binding behavior essential for rational drug

development and understanding biochemical mechanisms (Khan, Zakari, Zhang, Dagar, & Singh, 2022).

The study highlights promising compounds for targeting SNCA-related mechanisms in Parkinson's disease (PD), focusing on ligands that modulate SNCA expression, prevent aggregation, and enhance aggregate clearance. Key candidates include curcumin, quercetin, myricetin, fisetin, and genistein, which inhibit aggregation and provide neuroprotection, along with existing PD treatments like levodopa, carbidopa, pramipexole, and selegiline, which address dopamine depletion and reduce oxidative stress (D. Wang et al., 2023). Emerging bioactive ligands such as ketoconazole, rutin, cilazapril, and benazepril demonstrated strong binding affinities with both native and mutant SNCA forms, offering potential therapeutic benefits.

Additionally, Protein-ligand interaction profiling further revealed distinct molecular interactions for these compounds, underscoring their significance as candidates for experimental validation in modulating SNCA aggregation and neurodegeneration in PD (Pusnik, Petrovski, & Lumi, 2022). Future advancements in the early detection, treatment, and prevention of Parkinson's disease (PD) are likely to arise from continued research on the SNCA gene. Promising developments include the identification of early biomarkers, targeted gene therapies, immunotherapies to inhibit alpha-synuclein aggregation, RNA-based treatments, and CRISPR gene editing. Additionally, personalized medicine approaches tailored to individual genetic profiles offer significant potential. Ongoing research into alpha-synuclein biology remains essential for translating these findings into effective clinical applications.

CONCLUSION

The alpha-synuclein protein (SNCA) is located on human chromosome 4, and plays a perilous role in early-onset Parkinson's disease (PD), where its accumulation in brain cells forms clumps known as Lewy bodies. Our computational research on nsSNPs has provided insights into how these mutations adversely affect the structure and function of the SNCA protein. Our study identified 17 highly detrimental nsSNPs in the SNCA gene, which significantly disrupt the alpha-synuclein protein, contributing to PD pathogenesis. Notably, mutations such as P138H and G36S exhibited substantial structural alterations, as indicated by high RMSD scores. Docking studies of native and mutant proteins with selected compounds (Ketoconazole, Rutin, Cilazapril, Benazepril, Hesperidin, and Paeoniflorin) revealed potential therapeutic interactions, suggesting that these nsSNPs could serve as valuable targets for future drug discovery. This research not only enhances our understanding of the molecular mechanisms underlying PD but also paves the way for the development of targeted therapies.

ACKNOWLEDGMENT

We would like to express our sincere gratitude to our supervisor, Dr. Muhammad Saleem, for his invaluable guidance

Author Contribution

Not Applicable

Funding Information

No Funding

Declaration of Conflict

The authors declare that they have no known competing financial interests or personal relationships that could have appeared to influence the work reported in this paper.

REFERENCES

1. Antonova, L., Paramanathan, P., Falls, T., Wedge, M.-E., Mayer, J., Sekhon, H. S., . . . Bell, J. C.

- (2024). Molecular Characterization and Xenotransplantation of Pancreatic Cancer Using Endoscopic Ultrasound-Guided Fine Needle Aspiration (EUS-FNA). *Cancers*, 16(15), 2721.
2. Banerjee, A., Santra, D., & Maiti, S. (2020). Energetics and IC50 based epitope screening in SARS CoV-2 (COVID 19) spike protein by immunoinformatic analysis implicating for a suitable vaccine development. *Journal of Translational Medicine*, 18, 1-14.
 3. Beg, M. A., Hejazi, I. I., Thakur, S. C., & Athar, F. (2022). Domain-wise differentiation of *Mycobacterium tuberculosis* H37Rv hypothetical proteins: A roadmap to discover bacterial survival potentials. *Biotechnology and applied biochemistry*, 69(1), 296-312.
 4. Binotti, B., Jahn, R., & Pérez-Lara, Á. (2021). An overview of the synaptic vesicle lipid composition. *Archives of Biochemistry and Biophysics*, 709, 108966.
 5. Blauwendraat, C., Makarious, M. B., Leonard, H. L., Bandres-Ciga, S., Iwaki, H., Nalls, M. A., . . . Singleton, A. B. (2021). A population scale analysis of rare SNCA variation in the UK Biobank. *Neurobiology of disease*, 148, 105182.
 6. Bloem, B. R., Okun, M. S., & Klein, C. (2021). Parkinson's disease. *The Lancet*, 397(10291), 2284-2303.
 7. Bouqdayr, M., Abbad, A., Baba, H., Saih, A., Wakrim, L., & Kettani, A. (2023). Computational analysis of structural and functional evaluation of the deleterious missense variants in the human CTLA4 gene. *Journal of Biomolecular Structure and Dynamics*, 41(23), 14179-14196.
 8. Brás, J., Gibbons, E., & Guerreiro, R. (2021). Genetics of synucleins in neurodegenerative diseases. *Acta Neuropathologica*, 141, 471-490.
 9. Caramiello, A. M., & Pirota, V. (2024). Novel Therapeutic Horizons: SNCA Targeting in Parkinson's Disease. *Biomolecules*, 14(8), 949.
 10. Costa, B. (2022). Integration of in silico and in vitro approaches to investigate genetic and functional drivers of frontotemporal lobar degeneration. UCL (University College London).
 11. D'Addio, F., Lazzaroni, E., Lunati, M. E., Preziosi, G., Ercolanoni, M., Turola, G., . . . Scarioni, S. (2024). Vaccinome Landscape in Nearly 620 000 Patients With Diabetes. *The Journal of Clinical Endocrinology & Metabolism*, dgae476.
 12. Dorsey, E. R., & Bloem, B. R. (2024). Parkinson's disease is predominantly an environmental disease. *Journal of Parkinson's Disease*, 14(3), 451-465.
 13. Du, T., Wang, L., Liu, W., Zhu, G., Chen, Y., & Zhang, J. (2021). Biomarkers and the Role of α -Synuclein in Parkinson's Disease. *Frontiers in aging neuroscience*, 13, 645996.
 14. Fakhree, M. A., Konings, I. B., Kole, J., Cambi, A., Blum, C., & Claessens, M. M. (2021). The localization of alpha-synuclein in the endocytic pathway. *Neuroscience*, 457, 186-195.
 15. Ghasemi, S., Mahdavi, M., Maleki, M., Salahshourifar, I., & Kalayinia, S. (2022). A novel likely pathogenic variant in the FBXO32 gene associated with dilated cardiomyopathy according to whole-exome sequencing. *BMC Medical Genomics*, 15(1), 234.
 16. Grewal, A. K., Singh, T. G., Sharma, D., Sharma, V., Singh, M., Rahman, M. H., . . . Albadrani, G. M. (2021). Mechanistic insights and perspectives involved in neuroprotective action of quercetin. *Biomedicine & Pharmacotherapy*, 140, 111729.
 17. Guan, Y., Zhao, X., Liu, F., Yan, S., Wang, Y., Du, C., . . . Zhang, C. X. (2020). Pathogenic Mutations Differentially Regulate Cell-to-Cell Transmission of α -Synuclein. *Front Cell Neurosci*, 14, 159. doi:10.3389/fncel.2020.00159
 18. Guo, J., Wang, J., Sun, W., & Liu, X. (2022). The advances of post-stroke depression: 2021 update. *Journal of neurology*, 1-14.
 19. Huang, B., Kong, L., Wang, C., Ju, F., Zhang, Q., Zhu, J., . . . Bu, D. (2023). Protein Structure Prediction: Challenges, Advances, and the Shift of Research Paradigms. *Genomics Proteomics Bioinformatics*, 21(5), 913-925. doi:10.1016/j.gpb.2022.11.014
 20. Jumper, J., Evans, R., Pritzel, A., Green, T., Figurnov, M., Ronneberger, O., . . . Potapenko, A. (2021). Highly accurate protein structure prediction with AlphaFold. *nature*, 596(7873), 583-589.
 21. Kalia, A. (2024). Promoter share pledging and dividend payouts in India: does family involvement matters? *Asian Journal of Economics and Banking*.
 22. Keskin Karakoyun, H., Yüksel, Ş. K., Amanoglu, I., Naserikhojasteh, L., Yeşilyurt, A., Yakıcıer, C., . . . Akyerli, C. B. (2023). Evaluation of AlphaFold structure-based protein stability prediction on missense variations in cancer. *Frontiers in Genetics*, 14, 1052383.

23. Khalid, Z., & Naveed, H. (2022). Identification of destabilizing SNPs in SARS-CoV2-ACE2 protein and spike glycoprotein: implications for virus entry mechanisms. *Journal of Biomolecular Structure and Dynamics*, 40(3), 1205-1215.
24. Khan, I., Zakari, A., Zhang, J., Dagar, V., & Singh, S. (2022). A study of trilemma energy balance, clean energy transitions, and economic expansion in the midst of environmental sustainability: New insights from three trilemma leadership. *Energy*, 248, 123619.
25. Kondratyev, M. S., Rudnev, V. R., Nikolsky, K. S., Petrovsky, D. V., Kulikova, L. I., Malsagova, K. A., . . . Kaysheva, A. L. (2022). In silico study of the interactions of anle138b isomer, an inhibitor of amyloid aggregation, with partner proteins. *International journal of molecular sciences*, 23(24), 16096.
26. Kumar, A., Tamjar, J., Waddell, A. D., Woodroof, H. I., Raimi, O. G., Shaw, A. M., . . . van Aalten, D. M. (2017). Structure of PINK1 and mechanisms of Parkinson's disease-associated mutations. *Elife*, 6. doi:10.7554/eLife.29985
27. Legito, L., & Andriani, E. (2023). Emerging Technologies and Marketing Strategy: A Bibliometric Review of Digital Marketing and Innovation. *The Eastasouth Journal of Information System and Computer Science*, 1, 13-24. doi:10.58812/esiscs.v1i01.130
28. Lim, S.-Y., & Klein, C. (2024). Parkinson's disease is predominantly a genetic disease. *Journal of Parkinson's Disease*(Preprint), 1-16.
29. Liu, Y., Singleton, A., Arribas-Bel, D., & Chen, M. (2021). Identifying and understanding road-constrained areas of interest (AOIs) through spatiotemporal taxi GPS data: A case study in New York City. *Computers, Environment and Urban Systems*, 86, 101592.
30. Magistrelli, L., Contaldi, E., & Comi, C. (2021). The impact of snca variations and its product alpha-synuclein on non-motor features of parkinson's disease. *Life*, 11(8), 804.
31. Marsal-García, L., Urbizu, A., Arnaldo, L., Campdelacreu, J., Vilas, D., Ispierto, L., . . . Beyer, K. (2021). Expression levels of an alpha-synuclein transcript in blood may distinguish between early dementia with lewy bodies and parkinson's disease. *International journal of molecular sciences*, 22(2), 725.
32. Matthews, C. E., Patel, S., Saint-Maurice, P., Loftfield, E., Keadle, S. K., Chen, K. Y., . . . Berrigan, D. (2023). Physical Activity Levels (PAL) in United States Adults–2019. *Medicine and science in sports and exercise*, 55(5), 884.
33. Menon, P. J., Sambin, S., Criniere-Boizet, B., Courtin, T., Tesson, C., Casse, F., . . . French Parkinson disease Genetics Study, G. (2024). Genotype–phenotype correlation in PRKN-associated Parkinson's disease. *npj Parkinson's Disease*, 10(1), 72. doi:10.1038/s41531-024-00677-3
34. Morato Torres, C. A., Wassouf, Z., Zafar, F., Sastre, D., Outeiro, T. F., & Schüle, B. (2020). The Role of Alpha-Synuclein and Other Parkinson's Genes in Neurodevelopmental and Neurodegenerative Disorders. *Int J Mol Sci*, 21(16). doi:10.3390/ijms21165724
35. Palani, K. N., Deivasigamani, K., Piramanayagam, S., & Murthy, V. (2023). Drug Repurposing and Computational Drug Discovery for Aging and Neurological Disorders Drug Repurposing and Computational Drug Discovery (pp. 191-241): Apple Academic Press.
36. Paulékas, E., Vanagas, T., Lagunavičius, S., Pajėdienė, E., Petrikonis, K., & Rastenytė, D. (2024). Navigating the Neurobiology of Parkinson's: The Impact and Potential of α -Synuclein. *Biomedicines*, 12(9).
37. Pusnik, A., Petrovski, G., & Lumi, X. (2022). Dysphotopsias or unwanted visual phenomena after cataract surgery. *Life*, 13(1), 53.
38. Reddy, A., Reddy, R. P., Roghani, A. K., Garcia, R. I., Khemka, S., Pattoor, V., . . . Sehar, U. (2024). Artificial Intelligence in Parkinson's Disease: Early Detection and Diagnostic Advancements. *Ageing Research Reviews*, 102410.
39. Richard, M., Paul, C., Nijsten, T., Gisondi, P., Salavastru, C., Taieb, C., . . . Team, E. B. o. S. D. P. (2022). Prevalence of most common skin diseases in Europe: a population-based study. *Journal of the European Academy of Dermatology and Venereology*, 36(7), 1088-1096.
40. Rodrigues, C. H., Pires, D. E., & Ascher, D. B. (2021). DynaMut2: Assessing changes in stability and flexibility upon single and multiple point missense mutations. *Protein Science*, 30(1), 60-69.
41. Shaik, N. A., Al-Shehri, N., Athar, M., Awan, A., Khalili, M., Al Mahadi, H. B., . . . Awan, Z. (2023). Protein structural insights into a rare PCSK9 gain-of-function variant (R496W) causing familial hypercholesterolemia in a Saudi family: whole exome sequencing and computational analysis. *Front*

- Physiol, 14, 1204018. doi:10.3389/fphys.2023.1204018
42. Sharma, A., Osato, N., Liu, H., Asthana, S., Dakal, T. C., Ambrosini, G., . . . Wüllner, U. (2019). Common genetic variants associated with Parkinson's disease display widespread signature of epigenetic plasticity. *Scientific Reports*, 9(1), 18464. doi:10.1038/s41598-019-54865-w
 43. Singh, P., Kumar, V., Lee, K. W., & Hong, J. C. (2024). Discovery of Novel Allosteric SHP2 Inhibitor Using Pharmacophore-Based Virtual Screening, Molecular Docking, Molecular Dynamics Simulation, and Principal Component Analysis. *Pharmaceuticals (Basel)*, 17(7). doi:10.3390/ph17070935
 44. Skou, L. D., Johansen, S. K., Okarmus, J., & Meyer, M. (2024). Pathogenesis of DJ-1/PARK7-Mediated Parkinson's Disease. *Cells*, 13(4). doi:10.3390/cells13040296
 45. Sultana, T., Mou, S. I., Chatterjee, D., Faruk, M. O., & Hosen, M. I. (2024). Computational exploration of SLC14A1 genetic variants through structure modeling, protein-ligand docking, and molecular dynamics simulation. *Biochemistry and Biophysics Reports*, 38, 101703.
 46. Sykes, J., Holland, B., & Charleston, M. (2022). Unattained geometric configurations of secondary structure elements in protein structural space. *J Struct Biol*, 214(3), 107870. doi:10.1016/j.jsb.2022.107870
 47. Tanshee, R. R., Mahmud, Z., Nabi, A. N., & Sayem, M. (2024). A comprehensive in silico investigation into the pathogenic SNPs in the RTEL1 gene and their biological consequences. *Plos one*, 19(9), e0309713.
 48. Thomas, P. D., Ebert, D., Muruganujan, A., Mushayahama, T., Albou, L. P., & Mi, H. (2022). PANTHER: Making genome-scale phylogenetics accessible to all. *Protein Science*, 31(1), 8-22.
 49. Wang, D., Guerra, A., Wittke, F., Lang, J. C., Bakker, K., Lee, A. W., . . . Chen, Y.-H. (2023). Real-time monitoring of infectious disease outbreaks with a combination of Google Trends search results and the moving epidemic method: A respiratory syncytial virus case study. *Tropical Medicine and Infectious Disease*, 8(2), 75.
 50. Wang, J., Shi, Y., Zhou, H., Zhang, P., Song, T., Ying, Z., . . . Zeng, X. (2022). piRBase: integrating piRNA annotation in all aspects. *Nucleic acids research*, 50(D1), D265-D272.
 51. Wassouf, Z., Hentrich, T., Samer, S., Rotermund, C., Kahle, P. J., Ehrlich, I., . . . Schulze-Hentrich, J. M. (2018). Environmental Enrichment Prevents Transcriptional Disturbances Induced by Alpha-Synuclein Overexpression. *Front Cell Neurosci*, 12, 112. doi:10.3389/fncel.2018.00112
 52. Watt, K. J. C., Meade, R. M., Williams, R. J., & Mason, J. M. (2022). Library-Derived Peptide Aggregation Modulators of Parkinson's Disease Early-Onset α -Synuclein Variants. *ACS Chem Neurosci*, 13(12), 1790-1804. doi:10.1021/acchemneuro.2c00190
 53. Wayment-Steele, H. K., Ojoawo, A., Otten, R., Apitz, J. M., Pitsawong, W., Hömberger, M., . . . Kern, D. (2024). Predicting multiple conformations via sequence clustering and AlphaFold2. *nature*, 625(7996), 832-839.
 54. Weisheit, I., Kroeger, J. A., Malik, R., Klimmt, J., Crusius, D., Dannert, A., . . . Paquet, D. (2020). Detection of deleterious on-target effects after HDR-mediated CRISPR editing. *Cell reports*, 31(8).
 55. Wolff, J. (2023). *An introduction to political philosophy*: Oxford University Press.
 56. Wright, C. F., Campbell, P., Eberhardt, R. Y., Aitken, S., Perrett, D., Brent, S., . . . Lindsay, S. J. (2023). Genomic diagnosis of rare pediatric disease in the United Kingdom and Ireland. *New England Journal of Medicine*, 388(17), 1559-1571.
 57. Yazar, M., & Özbek, P. (2021). In silico tools and approaches for the prediction of functional and structural effects of single-nucleotide polymorphisms on proteins: an expert review. *OMICS: A Journal of Integrative Biology*, 25(1), 23-37.